SUPPORTING INFORMATION

Enantiomorphic single component conducting nickel(II) and platinum(II) bis(diethyl-dddt) crystalline complexes†

Alexandre Abhervé,*[a] Nabil Mroweh,[a] HengBo Cui,[b] Reizo Kato,[b] Nicolas Vanthuyne,[c] Pere Alemany,[d] Enric Canadell*[e,f] and Narcis Avarvari*[a]

[a] *MOLTECH-Anjou, UMR 6200, CNRS, UNIV Angers, 2 bd Lavoisier, 49045 ANGERS Cedex, France. E-mail: alexandre.abherve@univ-angers.fr; narcis.avarvari@univ-angers.fr*

[b] *Condensed Molecular Materials Laboratory, RIKEN, 2-1 Hirosawa, Wako, Saitama 351-0198, Japan*

[c] *Aix Marseille Univ, CNRS, Centrale Med, FSCM, Marseille, France*

[d] *Departament de Ciència de Materials i Química Física and Institut de QuímicaTeòrica i Computacional (IQTCUB), Universitat de Barcelona, Martí i Franquès 1, 08028 Barcelona, Spain*

[e] *Institut de Ciència de Materials de Barcelona, ICMAB-CSIC, Campus de la UAB, E-08193, Bellaterra, Spain. E-mail: canadell@icmab.es*

[f] *Royal Academy of Sciences and Arts of Barcelona, Chemistry Section, La Rambla 115, 08002 Barcelona, Spain*

† Electronic supplementary information (ESI) available. CCDC 2386847–2386851. For ESI and crystallographic data in CIF or other electronic format see DOI:10.1039/XXXXX

Chiral HPLC

Analytical chiral HPLC separation for compound (*rac*)-**de-dddt-1,3-dithiole-2-thione**

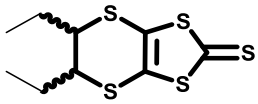

• The sample is dissolved in dichloromethane, injected on the chiral column, and detected with an UV detector at 254 nm and a circular dichroism detector at 254 nm. The flow-rate is 1 mL/min.

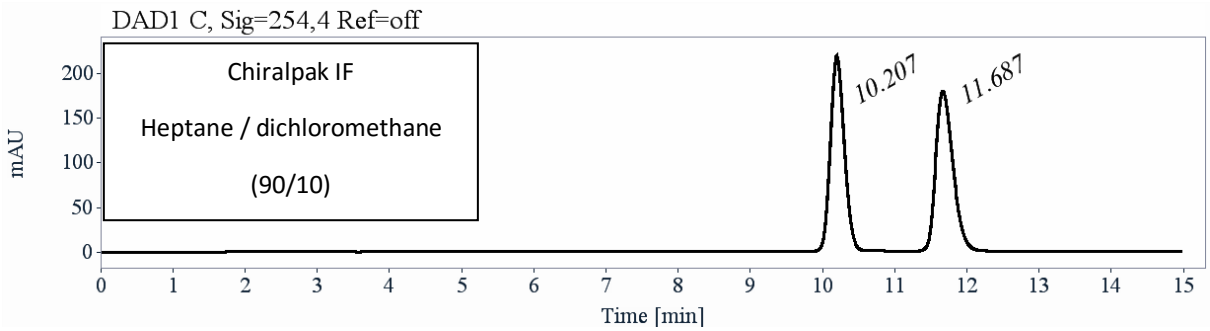

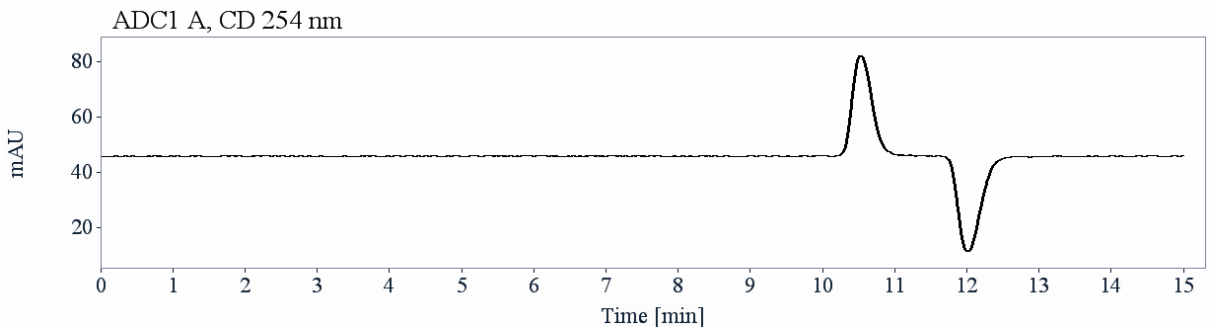

RT [min]	Area	Area%	Capacity Factor	Enantioselectivity	Resolution (USP)
10.21	2984	49.81	2.46		
11.69	3006	50.19	2.96	1.20	3.71
Sum	5991	100.00			

Fig. S1 Analytical chiral HPLC separation for compound (*rac*)-**de-dddt-1,3-dithiole-2-thione**.

Preparative separation for compound (*rac*)-**de-dddt-1,3-dithiole-2-thione**:

• Sample preparation: About 235 mg of compound **(*rac*)-de-dddt-1,3-dithiole-2-thione** are dissolved in 17 mL of a mixture of hexane and dichloromethane (64/36).

• Chromatographic conditions: Chiralpak IF (250 x 10 mm), hexane / dichloromethane (90/10) as mobile phase, flow-rate = 5 mL/min, UV detection at 254 nm.

• Injections (stacked): 190 times 90 µL, every 5 minutes.

• First fraction: 100 mg of the first eluted ((+, CD 254nm)-enantiomer) with ee > 96.5%

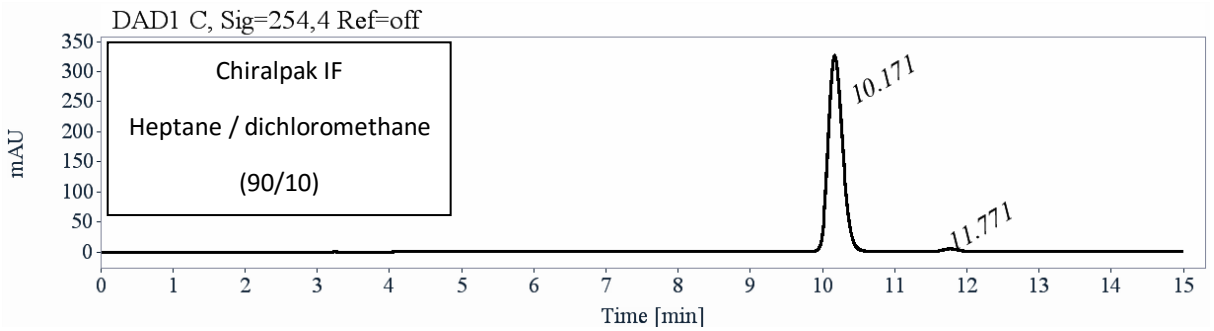

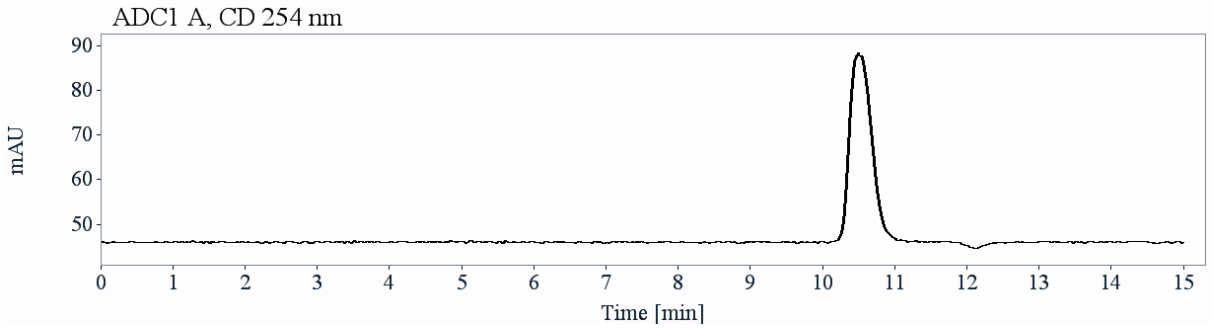

RT [min]	Area	Area%
10.17	4514	98.39
11.77	74	1.61
Sum	4588	100.00

Fig. S2 Chiral HPLC separation for compound (*R,R*)- **de-dddt-1,3-dithiole-2-thione**.

• Second fraction: 95 mg of the second eluted ((-, CD 254 nm)-enantiomer) with ee > 99.5%

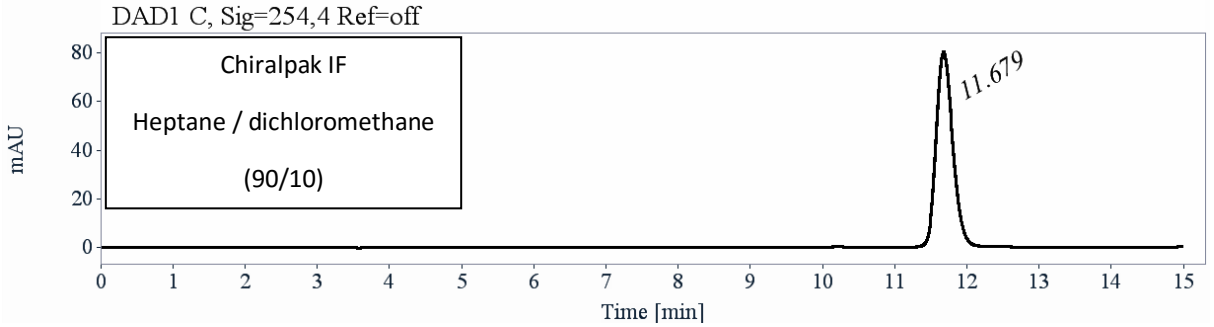

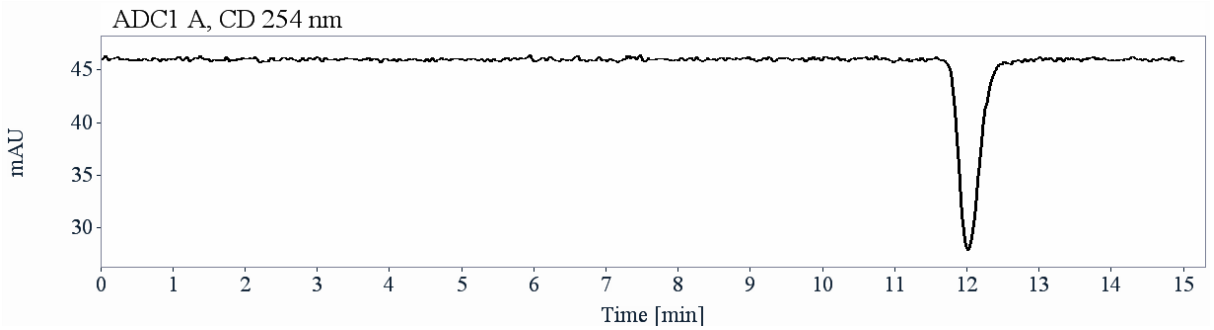

RT [min]	Area	Area%
11.68	1288	100.00
Sum	1288	100.00

Fig. S3 Chiral HPLC separation for compound (*S,S*)- **de-dddt-1,3-dithiole-2-thione**.

Optical rotations

Optical rotations were measured on a Jasco P-2000 polarimeter with a sodium lamp (589 nm), a halogen lamp (578 nm and 546 nm), in a 10 cm cell, thermostated at 25°C with a Peltier controlled cell holder.

λ (nm)	(*R*,*R*)-**de-dddt-1,3-dithiole-2-thione** first eluted on Chiralpak IF $[\alpha]_{\lambda}^{25}$ (CH_2Cl_2, c =0.13)	(*S*,*S*)-**de-dddt-1,3-dithiole-2-thione** second eluted on Chiralpak IF $[\alpha]_{\lambda}^{25}$ (CH_2Cl_2, c =0.13)
589	+ 527	- 538
578	+ 572	- 583
546	+ 824	- 839

Electronic Circular Dichroism (ECD) and UV-Visible spectroscopy

ECD and UV spectra were measured on a JASCO J-815 spectrometer equipped with a JASCO Peltier cell holder PTC-423 to maintain the temperature at 25.0 ± 0.2°C. A CD quartz cell of 1 mm of optical pathlength was used. The CD spectrometer was purged with nitrogen before recording each spectrum, which was baseline subtracted.
The baseline was always measured for the same solvent and in the same cell as the samples.
The spectra are presented without smoothing and further data processing.

(*R,R*)- **de-dddt-1,3-dithiole-2-thione**, first eluted on Chiralpak IF: green solid line, concentration = 1.08 mmol.L^{-1} in acetonitrile.

(*S,S*)- **de-dddt-1,3-dithiole-2-thione**, second eluted on Chiralpak IF: red dotted line, concentration = 1.09 mmol.L^{-1} in acetonitrile.

Acquisition parameters: 0.1 nm as intervals, scanning speed 50 nm/min, band width 1 nm, and 3 accumulations per sample.

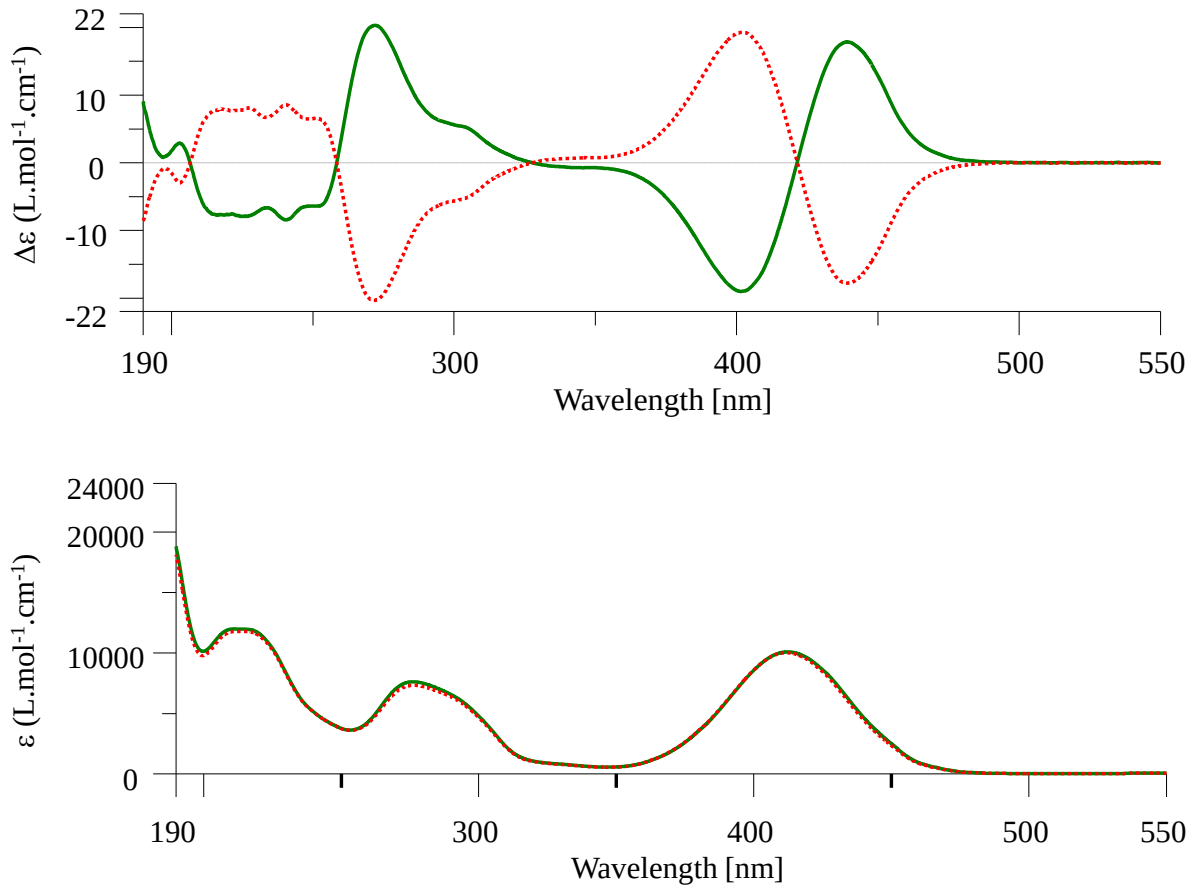

Fig. S4 CD (top) and UV-Vis (bottom) spectra of (*R,R*)- **de-dddt-1,3-dithiole-2-thione** (green line) and (*S,S*)- **de-dddt-1,3-dithiole-2-thione** (red dotted line).

X-ray crystallography

Table S1 Crystallographic data for **(TBA)[Ni(*S,S*-de-dddt)(*R,R*-de-dddt)]**

	(TBA) [Ni(*S,S*-dedddt)(*R,R*-dedddt)]
Empirical formula	$C_{32}H_{60}NNiS_8$
Fw	774.00
Crystal color	Green
Crystal size (mm^3)	0.05*0.05*0.01
Temperature (K)	150
Wavelength (Å)	1.54184
Crystal system, Z	Monoclinic, 4
Space group	$P2_1/c$
a (Å)	14.6673 (5)
b (Å)	17.9434 (3)
c (Å)	16.4154 (5)
α (°)	90
β (°)	115.109 (4)
γ (°)	90
V (Å³)	3911.97 (19)
ρ_{calc} ($g.cm^{-3}$)	1.314
μ(CuKα) (mm^{-1})	4.868
θ range (°)	3.328–73.662
Data collected	35475
Data unique	7798
Data observed	6623
R(int)	0.0389
Nb of parameters / restraints	382/13
$R1(F)$,[a] $I > 2\sigma(I)$	0.0619
$wR2(F^2)$,[b] all data	0.1677
$S(F^2)$,[c] all data	1.060
CCDC number	2386847

[a] $R1(F) = \Sigma\|\|F_0\|-\|F_C\|\|/\Sigma|F_0|$; [b] $wR2(F^2) = [\Sigma w(F_0^2-F_C^2)^2/\Sigma wF_0^4]^{1/2}$; [c] $S(F^2) = [\Sigma w(F_0^2-F_C^2)^2/(n+r-p)]^{1/2}$.

Table S2 Crystallographic data for **[Ni(*rac*-de-dddt)$_2$]**, **[Pt(*rac*-de-dddt)$_2$]**, **[Ni(*S,S*-de-dddt)$_2$]** and **[Pt(*R,R*-de-dddt)$_2$]**.

	[Ni(*rac*-dedddt)$_2$]	**[Pt(*rac*-dedddt)$_2$]**	**Ni(*S,S*-dedddt)$_2$]**	**[Pt(*R,R*-dedddt)$_2$]**
Empirical formula	$C_{32}H_{48}Ni_2S_{16}$	$C_{32}H_{48}Pt_2S_{16}$	$C_{16}H_{24}NiS_8$	$C_{16}H_{24}PtS_8$
Fw	1063.08	1335.84	531.54	667.92
Crystal color	Black	Black	Black	Black
Crystal size (mm^3)	0.08*0.08*0.04	0.2*0.03*0.02	0.3*0.1*0.05	0.07*0.06*0.02
Temperature (K)	150	150	150	150
Wavelength (Å)	1.54184	1.54154	1.54184	1.54154
Crystal system, Z	Tetragonal, 8	Tetragonal, 8	Tetragonal, 8	Tetragonal, 8
Space group	$P4_12_12$	$P4_12_12$	$P4_12_12$	$P4_32_12$
a (Å)	14.2738 (7)	14.3130 (4)	14.6382 (2)	14.7208 (2)
b (Å)	14.2738 (7)	14.3130 (4)	14.6382 (2)	14.7208 (2)
c (Å)	21.7030 (11)	21.7690 (7)	20.8242 (4)	20.8598 (5)
α (°)	90	90	90	90
β (°)	90	90	90	90
γ (°)	90	90	90	90
V (Å^3)	4421.8 (4)	4459.6 (2)	4462.15 (12)	4520.36 (14)
ρ_{calc} (g.cm^{-3})	1.597	1.990	1.582	1.963
μ(CuKα) (mm^{-1})	8.318	18.766	8.243	18.514
θ range (°)	3.71–73.37	3.70–73.55	3.69–73.60	3.67–73.99
Data collected	9610	16611	17730	37716
Data unique	4320	4430	4453	4531
Data observed	3300	3592	4176	4290
R(int)	0.0558	0.0447	0.0652	0.0953
Nb of parameters / restraints	232/0	232/0	227/0	227/0
Flack parameter	0.47 (11)	0.51 (4)	-0.01 (3)	-0.061 (18)
$R1(F)$,[a] $I > 2\sigma(I)$	0.0981	0.0505	0.0390	0.0445
$wR2(F^2)$,[b] all data	0.2900	0.1359	0.1060	0.1049
$S(F^2)$,[c] all data	1.027	1.036	1.046	1.043
CCDC number	2386848	2386849	2386850	2386851

[a] $R1(F) = \Sigma\|F_0|-|F_C\|/\Sigma|F_0|$; [b] $wR2(F^2) = [\Sigma w(F_0^2-F_C^2)^2/\Sigma wF_0^4]^{1/2}$; [c] $S(F^2) = [\Sigma w(F_0^2-F_C^2)^2/(n+r-p)]^{1/2}$.

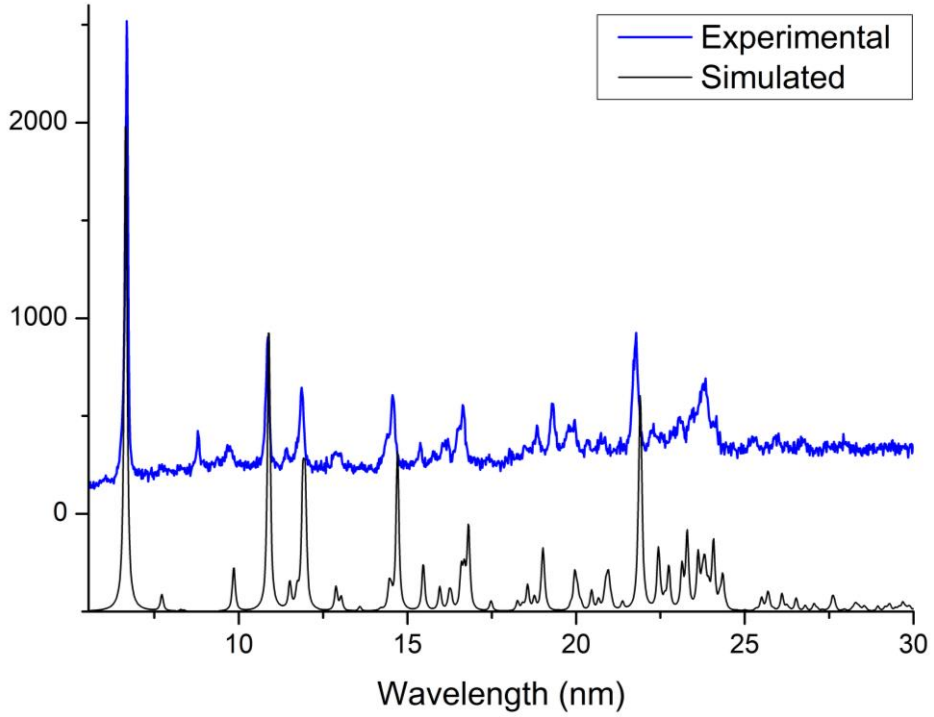

Fig. S5 Simulated and experimental X-ray powder diffractograms of (TBA)[Ni(*S*,*S*-de-dddt)(*R*,*R*-de-dddt)].

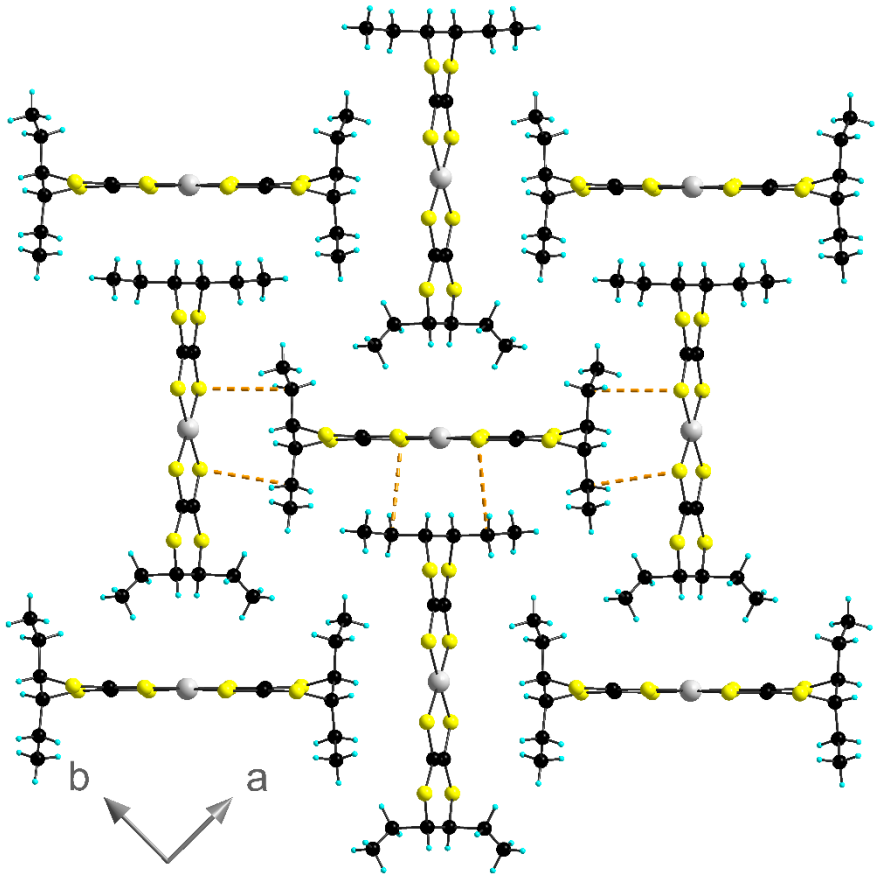

Fig. S6 View of one 2D layer from **[Pt(*rac*-de-dddt)$_2$]** in the *ab* plane. Intermolecular C-H···S interactions between the central and neighbouring complexes are represented in orange dashed lines.

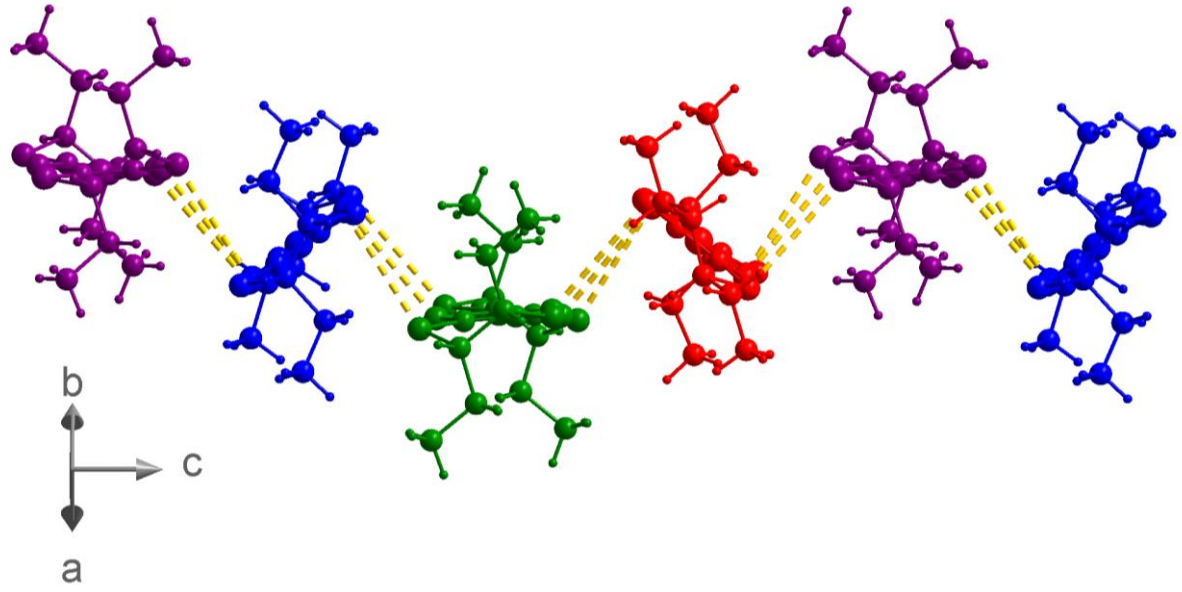

Fig. S7 "Out-of-plane" intermolecular S···S interactions between neighbouring complexes in **[Ni(*S,S*-de-dddt)$_2$]** along the *c* axis. Four colours are used to discriminate between the complexes belonging to the different ABCD layers.

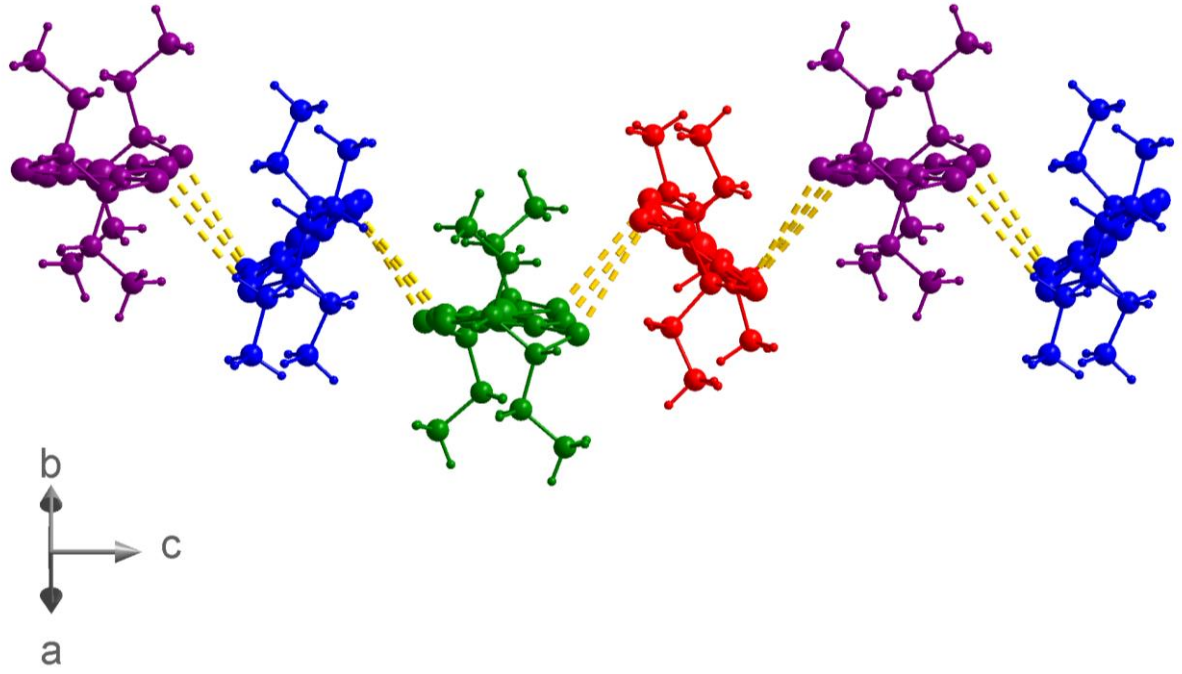

Fig. S8 "Out-of-plane" intermolecular S···S interactions between neighbouring complexes in **[Pt(*R,R*-de-dddt)$_2$]** along the *c* axis. Four colours are used to discriminate between the complexes belonging to the different ABCD layers.

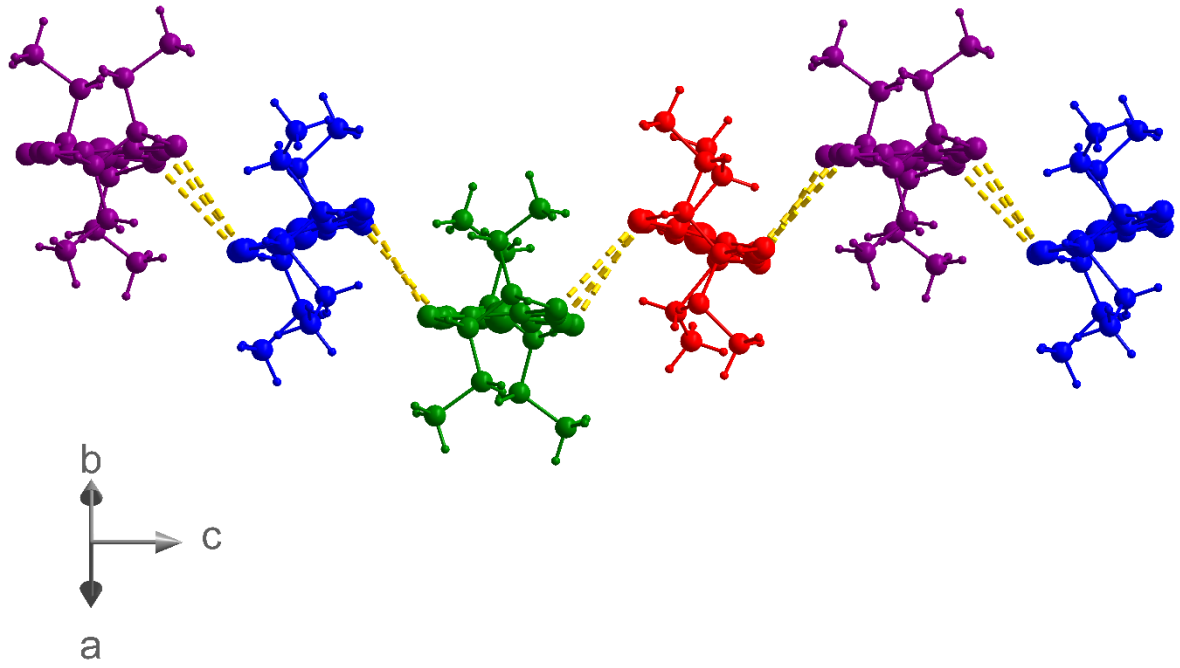

Fig. S9 "Out-of-plane" intermolecular S···S interactions between neighbouring complexes in **[Pt(*rac*-de-dddt)$_2$]** along the *c* axis. Four colours are used to discriminate between the complexes belonging to the different ABCD layers.

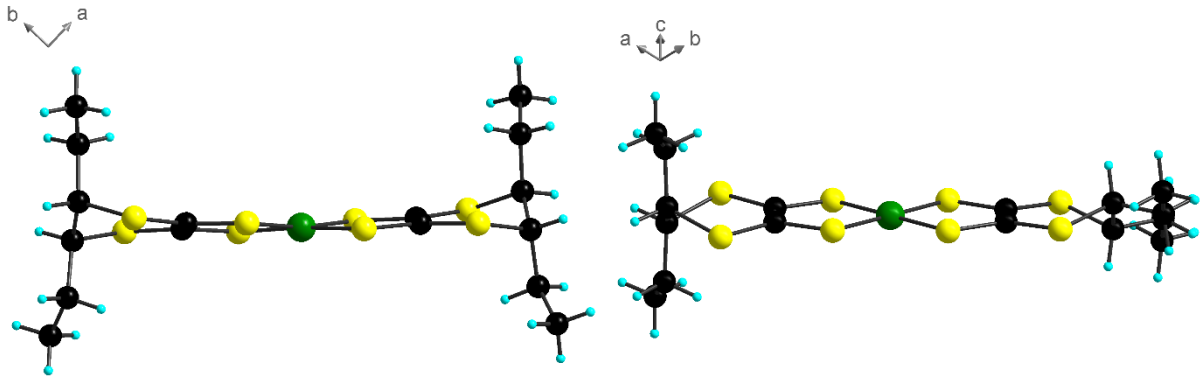

Complex 1 Complex 2

Fig. S10 The two independent complexes, with a highlight on the conformations of the ethyl groups, i.e. all-ax in 1 and (ax,ax,eq,eq) in 2, in the structure of [Ni(*S,S*-de-dddt)$_2$].

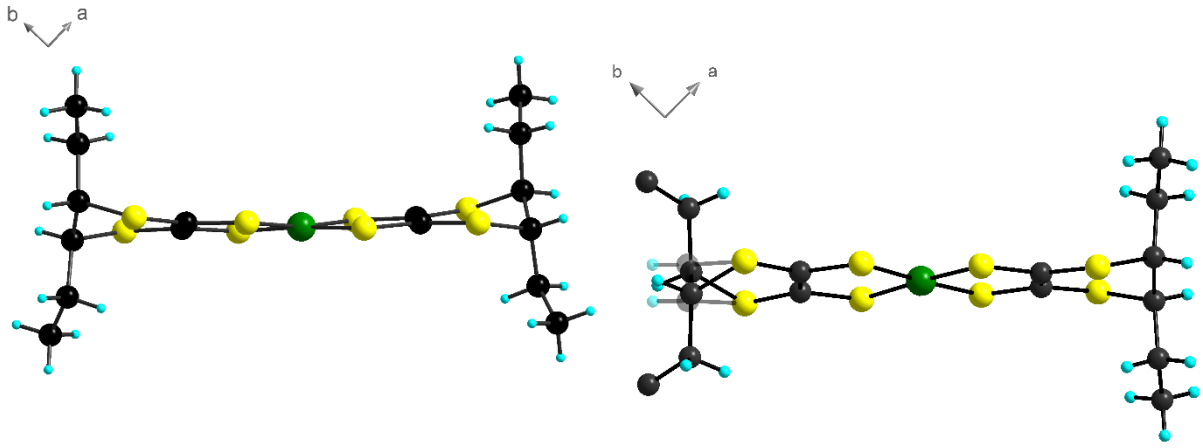

Complex 1 Complex 2

Fig. S11 The two independent complexes, with a highlight on the conformations of the ethyl groups, i.e. all-ax in 1 and in 2, in the structure of [Ni(*rac*-de-dddt)$_2$].

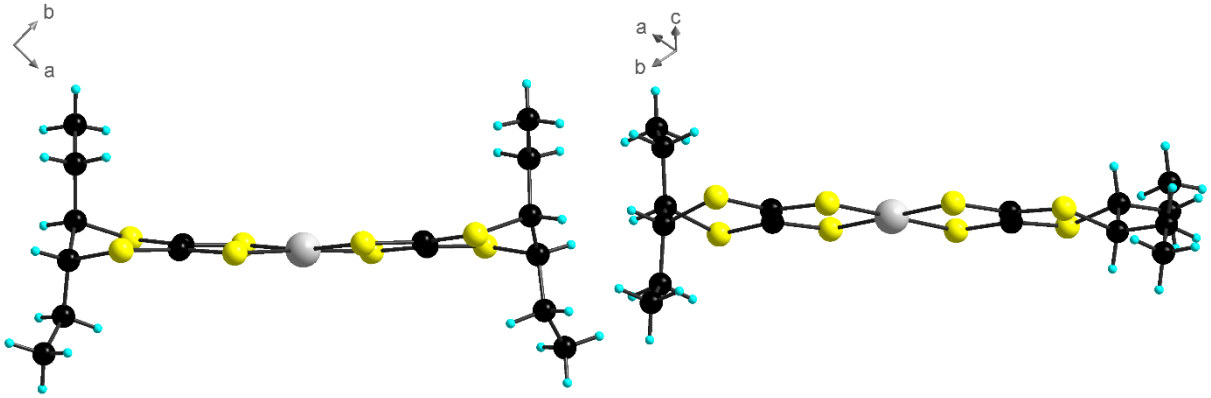

Complex 1 Complex 2

Fig. S12 The two independent complexes, with a highlight on the conformations of the ethyl groups, i.e. all-ax in 1 and (ax,ax,eq,eq) in 2, in the structure of [Pt(*R,R*-de-dddt)$_2$].

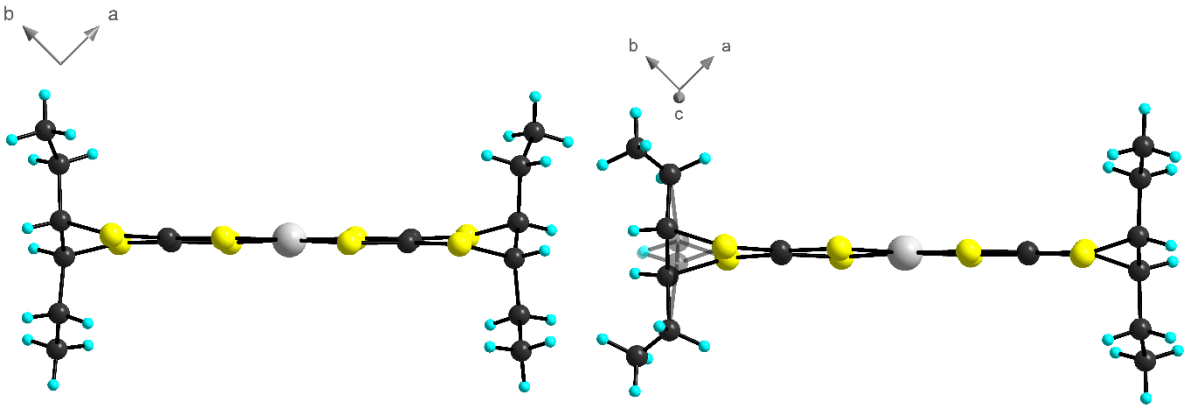

Complex 1 Complex 2

Fig. S13 The two independent complexes, with a highlight on the conformations of the ethyl groups, i.e. all-ax in 1 and in 2, in the structure of [Pt(*rac*-de-dddt)$_2$].

Band structure calculations

Table S3 Calculated absolute values of the $|\beta_{HOMO\text{-}HOMO}|$ and $|\beta_{LUMO\text{-}LUMO}|$ interaction energies (eV) for [Ni(*S*,*S*-de-dddt)$_2$], [Ni(*rac*-de-dddt)$_2$], [Pt(*R*,*R*-de-dddt)$_2$] and [Pt(*rac*-de-dddt)$_2$] at room temperature.

Compound	$\|\beta_{HOMO\text{-}HOMO}\|$ (eV)	$\|\beta_{LUMO\text{-}LUMO}\|$ (eV)
[Ni(*S*,*S*-de-dddt)$_2$]	I: 0.0744 II: 0.0065	I: 0.0187 II: 0.0071
[Ni(*rac*-de-dddt)$_2$]	I: 0.1106 II: 0.0063	I: 0.0671 II: 0.0032
[Pt(*R*,*R*-de-dddt)$_2$]	I: 0.0823 II : 0.0077	I: 0.0147 II: 0.0084
[Pt(*rac*-de-dddt)$_2$]	I: 0.1145 II : 0.0053	I: 0.0695 II: 0.0014